Biochimica et Biophysica Acta, 502 (1978) 61—79

BBA 47473

THEORY OF PROTON HYPERFINE INTERACTIONS IN BACTERIAL PHOTOSYNTHETIC SYSTEMS

BACTERIOPHEOPHYTIN CATION AND ANION

JANE C. CHANG and T.P. DAS

Department of Physics, State University of New York at Albany, Albany, N.Y. 12222 (U.S.A.)

(Received December 8th, 1977)

Summary

The electronic structures of the cation and anion of bacteriopheophytin *a* monomer are investigated by the self-consistent charge extended Hückel procedure including both π and σ electrons in the molecule. The calculated electron distributions are tested by comparison of the predicted hyperfine fields at proton sites with experimental data in both the ions and most important, by their ability to explain the observed trend in the hyperfine fields in going from the cation bacteriopheophytin$^+$ *a* to the anion, a trend that is similar in many respects to the corresponding observed trend for the bacteriochlorophyll *a* cation and anion. Good agreement is obtained with experiment both for the absolute values of the observed proton hyperfine fields in both bacteriopheophytin a cation and anion as well as the ratio of the corresponding fields for the two systems. In particular, our calculated electron distributions in the two molecules lead, for the cation, to substantially different proton hyperfine fields for the two methyl groups attached to rings I and III, while for the anion, the corresponding fields are much closer to each other, a trend in good agreement with recent data. Also explained are the features of larger methine hyperfine constants in the anion as compared to the cation and the reverse trend for the protons in rings II and IV. Other features of the calculated electron distributions in the cation and anion are discussed and compared with each other. Possible additional measurements in the two systems that could provide further tests of the theoretically obtained electron distribution will be pointed out.

Abbreviations: BPh *a*, bacteriopheophytin *a*. BChl *a*, bacteriochlorophyll *a*.

(I) Introduction

The bacteriochlorophyll dimer cation $(BChl)_2^+$ has recently been shown experimentally, particularly by electron paramagnetic resonance [1—4] (EPR) and electron-nuclear double resonance [5,6] (ENDOR) methods, to be the primary electron donor [7] in photosynthetic bacteria. Also from recent EPR and Mössbauer measurements, ubiquinone, magnetically coupled to a Fe^{2+} ion, has been shown [8,9] to be the primary electron acceptor. A number of basic questions remain to be answered for the understanding of the primary processes in bacterial photosynthesis. Thus the nature of the bonding between monomer units in $(BChl)_2^+$ dimer is not completely understood at the present time, although a number of theories [10—13] have been proposed for it. The molecular systems associated with intermediate states in the primary processes have not been completely understood as also the role of the bacteriopheophytin (BPh) molecules in the reaction center. It has recently been proposed [14] that bacteriopheophytin may be a transient electron acceptor in the *P*-870 oxidation process.

The understanding of these problems, particularly the nature of the bonding between monomer units to give the primary donor dimer, $(BChl)_2^+$ can be substantially assisted by a proper understanding of the electron distributions over the monomer units themselves. Recently, through the use [15—19] of EPR and ENDOR techniques on the monomer cations and anions of bacteriochlorophyll and bacteriopheophytin molecules and their selectively deuterated counterparts, information regarding the hyperfine fields has become available at the proton sites in the various monomers. These fields can be evaluated from calculated spin densities at the proton sites and can therefore act as valuable checks of the correctness of calculated wave-functions for these molecules.

The available data [15—18] on the proton hyperfine fields in the various monomer units have indicated interesting variations of the spin densities at pro-

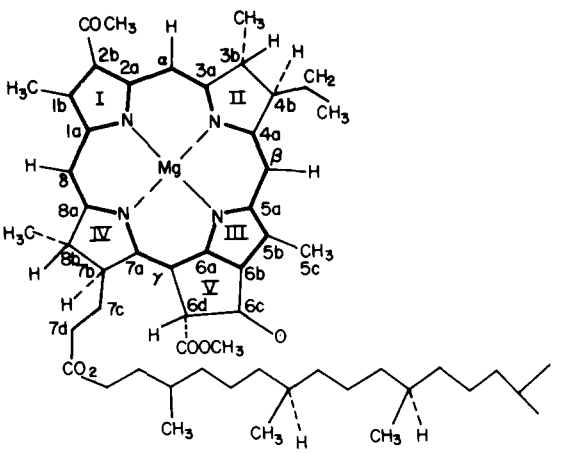

Fig. 1. Bacteriochlorophyll *a* molecule. The heavy lines represent the conjugation path used in earlier π-orbital calculations.

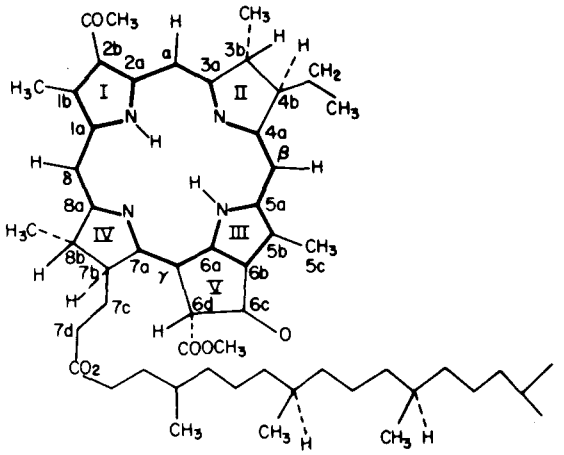

Fig. 2. Bacteriopheophytin *a* molecule. The heavy lines represent the conjugation path used in earlier π-orbital calculations.

ton sites over the monomer units themselves and also interesting changes in these distributions in going from cations to anions. The trends are very similar in going from the cations [15—17] $BChl^+$ *a* to the corresponding anions [18]. There are also much smaller, but nevertheless, finite variations [15,17,18] in going from $BChl^+$ *a* to BPh^+ *a* and from $BChl^-$ *a* to Bph^- *a* (the arrangement of atoms and groups in BChl *a* and BPh *a* molecules being shown in Figs. 1 and 2). These various trends may be summarized as follows. For both the $BChl^+$ *a* ion [15—17] and BPh^+ *a* ion [17], the hyperfine constants for the methine protons are found to be small, in the neighborhood of 1 MHz. The hyperfine constant associated with the protons of the methyl groups directly linked to ring I is next in order in magnitude and is about 5 MHz. The hyperfine constant for the methyl protons in ring III is about a factor of two larger than for ring I. The only other proton hyperfine constant observed is associated with the protons in rings II and IV and these are the largest, about 60% higher than that for the methyl protons in ring III. The anions of both $BChl^-$ *a* and BPh^- *a* show completely different features, with the methyl protons of rings I and III now having nearly equal hyperfine constants comparable with that for the ring III methyl protons in the cations. The methine protons are now found to have considerably larger hyperfine constants than in the cations, within 15% of the values for the methyl protons of rings I and III. In contrast, while the protons in rings II and IV had the largest hyperfine constants in the cations, they are the smallest in the anions, and the corresponding ENDOR patterns are as yet unresolved with anions. Finally, regarding the differences between BPh *a* and BChl *a* systems, there are small but finite differences between the methine proton hyperfine constants in the two systems in the cases of both the cations and anions, the BPh^+ *a* system appearing to have a somewhat smaller [17] methine proton hyperfine constant than $BChl^+$ *a*. Also the methyl proton hyperfine constants [18] for rings I and III in $BChl^-$ *a* monomer appear to be slightly larger than the counterparts in BPh^- *a*, especially for ring I.

The earlier theoretical efforts to understand the spin density distribution in

these systems utilized [20,21] π-orbital procedures *. In these calculations, a π-network involving carbon and nitrogen atoms in the part of the BChl *a* molecule (cation or anion) indicated by the dark line in Fig. 1 was used. These calculations gave the unpaired spin populations on the carbon and nitrogen atoms included in the π-network. Using empirical relations between the π-orbital spin populations on the carbon atoms and the spin densities on the neighboring hydrogen atoms either on the plane of the π-orbital network or off the plane, the proton hyperfine constants for the $BChl^+$ *a* have been estimated. These results explained a number of features [15—17] of the experimental data, the methine protons having the smallest hyperfine constant, the methyl proton hyperfine constants in rings I and III, the next in order and the proton hyperfine constants for the rings II and IV, the highest in magnitude. However, since the π-network handled the rings I and III as equivalent, the theoretical values of the methyl proton hyperfine constants in these rings came out [15] equal in contrast with experimental results [15—17].

Our work reported here was aimed at the explanation of the observed features of the proton hyperfine constants for [15,17] BPh^+ *a* and [18] BPh^- *a* ions. Of particular interest to us was the explanation of the feature involving the marked difference between the proton hyperfine constants in rings I and III of [17] BPh^+ *a* (and [15—17] $BChl^+$ *a*) in contrast to the closeness of the corresponding hyperfine constants for [18] BPh^- *a* (and [15,18] $BChl^-$ *a*) and of course also of the very significant differences in the unpaired spin distributions by the other observed proton hyperfine constants [17,18] in BPh^+ *a* and BPh^-*a* (and [15—17] $BChl^+$ *a* and [18] $BChl^-$ *a*). We have utilized the self-consistent charge extended Hückel procedure [22—24] to obtain the electronic wave-functions for the two systems, BPh^+ *a* and BPh^- *a*, and used the wave-functions to obtain the unpaired spin distributions over the two systems. The above procedure includes in the molecular orbital wave-functions both the π and σ electrons and the interaction among them and, therefore, allows the recognition of the difference between the rings I and III due to the presence of the non-planar ring V adjacent to ring III.

Our results for the unpaired spin distributions for the cation and anion will be seen to provide a satisfactory explanation of the observed difference [17] in the proton hyperfine constants of the methyl groups in rings I and III in the case of BPh^+ *a* and lead to corresponding hyperfine constants for BPh^- *a* which are much closer to each other than in the case of BPh^+ *a*, in agreement with the experimental trend [18]. Our calculated spin distributions also explain all the other observed features [15,17,18] including, in the cation case, the small hyperfine constants [17] for the methine protons and the expected relatively large ones for the protons in rings II and IV, from observed $BChl^+$ *a* data [15—17] and the reverse trend [18] in the anion. In fact, it will be shown that the cause for the different ratios of the proton hyperfine constants for rings I and III for the cation and anion is related to that for the differences in the

*Felton, R.H. (quoted by Feher, G. et al [15]) has attempted to explain differences between the two rings I and III by attaching carbonyl groups to these rings, but the difference obtained was minimal and much smaller than needed to explain the observed difference in the methyl proton hyperfine constant for the two rings.

trends of the methine protons and ring II and ring IV protons in the two cases.

We have studied BPh^+ *a* and BPh^- *a* in the present work, both because of the interesting data available [15,17,18] for these two systems and in contrast to the case of the corresponding bacteriochlorophyll systems, $BChl^+$ *a* and $BChl^-$ *a*, one does not have the orbitals of the central magnesium atom to consider, which simplifies the calculation. However, in view of the overall similarity of the experimental data in the [15—18] BChl *a* and BPh *a* systems [15,17,18], success in the explanation of the trends in the hyperfine constant data in the latter can be considered as indicative of expected success in explaining the data in the BChl *a* systems. In subsequent investigations, we plan to treat the $BChl^+$ *a* and $BChl^-$ *a* molecules by the same procedure as that used here to attempt to understand some of the small but significant differences between the proton hyperfine constants, between the BChl *a* and BPh *a* ions, in particular the somewhat larger methine hyperfine constant observed in [16,17] $BChl^+$ *a* as compared to [17] BPh^+ *a*.

In Section II we discuss briefly the model system closely resembling BPh^- *a* molecule that we have used in our work, the modifications corresponding to the model system being made to keep the computational work practicable without any loss of physical insight. The methods for calculating the energy levels and wave-functions and obtaining spin densities and proton hyperfine constants from them is also briefly described in Section II. Section III presents our results for the spin density distributions in the cation and anion and the proton hyperfine constants. The results are compared with experiment [15,17,18] and the significance of the results and the nature of the agreement between theory and experiment is discussed. The final section, Section IV, presents concluding remarks and lists future theoretical and experimental investigations that could further enhance the understanding of the electronic structures of bacteriochlorophyll and bacteriopheophytin systems.

(II) Procedure of calculation of energy levels, wave-functions and proton hyperfine interactions constants

The model system used to carry out our calculations is shown in Fig. 3, and as can be seen from this figure, this model compound has most of the features

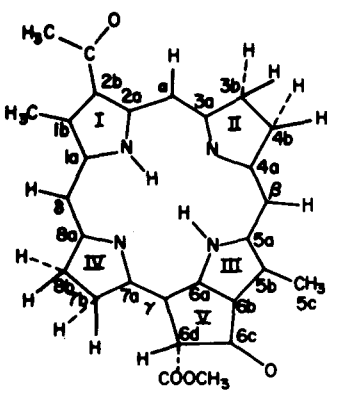

Fig. 3. Model system used in the present work for calculations on bacteriopheophytin *a* cation and anion.

of the BPh *a* system in Fig. 2 intact including the rings I through V. The main changes are the replacement of a number of groups by hydrogen atoms. These groups are the following: the methyl group attached to carbon site 3b in ring II, the ethyl group attached to the carbon atom at 4b, the phytyl group attached to the carbon atom at 7b, the methyl group attached to the carbon atom at site 8b and the methyl group in $COOCH_3$ in ring V. These changes, which correspond essentially to replacing single bonds C-C by C-H, are not expected to have any significant influence over the electron distribution over the rings I through V, particularly the spin densities at the proton sites whose hyperfine constants have been observed. However, they allow us to reduce the number of atoms and atomic orbitals involved to a practicable number. With the choice of the model system in Fig. 3, we have 59 atoms and 164 orbitals in our calculations, which include the ls orbitals on the hydrogen atoms and the 2s, $2p_x$, $2p_y$ and $2p_z$ orbitals on carbon, nitrogen and oxygen atoms. In the BPh^+ *a* system, we have a total of 175 electrons with 174 electrons doubly occupying 87 molecular energy levels of the system and one unpaired electron singly occupying one level. In the BPh^- *a* system, on the other hand, the total number of electrons is 177, 176 of these doubly occupying 88 molecular energy levels with one electron again having its spin unpaired. The locations of the atoms used in Fig. 3 for our model system are obtained from the crystal structure data in methyl pheophorbide a [25] and the use of conventional [26,27] bond distances and bond angles involving the C-H bonds where they are not known in the molecule because the positions of the hydrogen are not known from X-ray diffraction data. It is important to note, however, that the carbon atom frame work in ring II is planar in the pheophorbide structure since this ring is unsaturated there, whereas in bacteriochlorophyll and bacteriopheophytin systems, it is saturated. Consequently the bond distances and angles involving the lines joining the carbon atoms 3a, 3b, 4a and 4b are somewhat different for the bacteriopheophytin system than for pheophorbide. Since structural data regarding the positions of atoms are not available for the bacteriopheophytin system, we have used the carbon atomic positions in ring II as characteristic of pheophorbide. A change from this would have required modifications in quite a number of C-C bond distances and bond angles. The effect of the choice made for the geometry in ring II on the proton hyperfine constants associated with this ring shall be discussed in Section III dealing with the results of calculation for the hyperfine constants.

(A) Brief description of procedure of calculation of energy levels and wavefunctions

The elctronic wave-functions and energy levels of the cation and anion of the BPh *a* model system in Fig. 3 were obtained by the self-consistent charge-extended Hückel procedure [22]. This procedure is discussed in the literature [22—24] at a number of places. Only a brief description is included here for the sake of completeness. The molecular orbitals ϕ_μ, as in all semi-empirical procedures, are expressed as a linear combination of atomic orbitals χ_i in the form

$$\phi_\mu = \sum_i C_{\mu i}\chi_i \qquad (1)$$

the molecular orbital energies E_μ and the corresponding sets of coefficients $C_{\mu i}$ being obtained by variational principle, leading to the simultaneous linear equations:

$$\sum_j C_{\mu j}(h_{ij} - E_\mu S_{ij}) = 0 \tag{2}$$

which in turn yield the secular determinatal equation:

$$Det\,|h_{ij} - E_\mu S_{ij}| = 0 \tag{3}$$

In Eqns. 2 and 3, S_{ij} and h_{ij} represent the matrix elements of unity operator (overlap integrals) and the Hamiltonian, respectively. In this procedure, the matrix elements h_{ij} are approximated [22] by the following forms:

$$h_{ii} = h_{ii}^{o} + |q_l|\,(h_{ii}^{\pm}) \tag{4}$$

$$h_{ij} = \frac{\kappa}{2} S_{ij}(h_{ii} + h_{jj}) \tag{5}$$

where h_{ii}^{o}, h_{ii}^{+} and h_{ii}^{-} refer to the ionization energies for the electron in orbital χ_i for the atom l when it is neutral or carries single positive or negative charges, respectively. The value of the parameter $\kappa = 1.89$ has been found [23] from work on several metal-porphyrin systems to give the best fit between observed optical spectral data and those calculated from the energy levels of the corresponding systems. The charges q_l refer to the lth atom and are given in Mulliken's approximation [28] by the relation:

$$q_l = -\sum_\mu \sum_{i(l)} [|C_{\mu i}|^2 + \sum_{j(m)} C_{\mu i} C_{\mu j} S_{ij}] + Z_l \tag{6}$$

the symbol $i(l)$ indicating that the summation over i is carried out for those orbitals which are on atom l. Since q_l depends on the molecular orbital coefficients $C_{\mu i}$, the latter in turn being determinated from the Eqns. 2, which depends on the q_l-dependent matrix elements h_{ii} and h_{ij} (given in Eqns. 4 and 5), the process of calculation has to be carried out self-consistently. In our work, we have used the self-consistency limit for q_l as 0.05.

(B) Procedure for evaluation of hyperfine constants

The hyperfine spin Hamiltonian used for analyzing the EPR and ENDOR spectra is given by [29]

$$H^{spin} = \sum_l A_l \vec{I}_l \cdot \vec{S} + \sum_l \vec{I}_l \cdot \vec{\vec{B}}_l \cdot \vec{S} \tag{7}$$

In Eqn. 7, $\vec{I}_l$ and $\vec{S}$ are the vectors representing the spin of the nucleus atom l and the total electronic spin of the molecule. A_l refers to the isotropic hyperfine constant for the nucleus l, arising from the contact interaction [30,31] between the nuclear and electronic spin magnetic moments, the dipolar inter-

action between them leading to the tensor term $\vec{\vec{B}}_l$. In the liquid state, the effect of $\vec{\vec{B}}_l$ vanishes due to the random reorientational motion of the molecules and only the isotropic constants A_l are observed. In the solid state, the directional dependence of the dipolar spin-Hamiltonian leads to a broadening of the EPR and ENDOR spectra and again only the isotropic hyperfine interaction terms A_l are determined from these spectra. To determine $\vec{\vec{B}}_l$, single crystal measurements are desirable. From the contact term [30,31] in the basic hyperfine interaction Hamiltonian between the electronic and nuclear moments, the hyperfine constant A_l in Hertz can be related to the densities of the unpaired spin orbitals at the nucleus of atom according to the relation [31]:

$$A_l = \frac{2\gamma_e\gamma_l\hbar}{3S} \sum_{\substack{\mu \\ \text{unpaired}}} |\phi_\mu(l)|^2 \tag{8}$$

where γ_e and γ_l refer to the gyromagnetic ratios of the electron and lth nucleus, respectively, $\frac{1}{2}\gamma_e h$ and $\gamma_l I h$ being the Bohr magneton and the magnetic moment of the lth nucleus. For BPh^+ a and BPh^- a, there is only one unpaired electron and $S = \frac{1}{2}$, hence

$$A_l = \frac{4\gamma_e\gamma_l\hbar}{3} |\phi_{\text{unpaired}}(l)|^2 \tag{9}$$

For the protons of interest to us for which the hyperfine constants have been measured, namely, the protons attached to the carbon atoms 3b, 4b, 7b and 8b in rings II and IV, the methine protons attached to the α, β and δ carbon atoms and the protons in the methyl groups attached to carbon atoms 1b and 5b in rings I and III, we could thus get the hyperfine constants by evaluating $\phi_{\text{unpaired}}(l)$ at each of these protons. However, there are two complications, especially for the methine and methyl group protons. Thus, there is an important effect present which is particularly significant when the direct contribution to the hyperfine constant is small, as in the case of the methine protons, where the density at the proton sites from the π-type unpaired electron would vanish if the molecule had planar geometry especially at the sites of the methine groups. The pertinent important effect in this case is the exchange polarization effect [31—35] involving the exchange interaction between the unpaired spin electron and the electrons in the occupied paired spin states which makes the space parts of the wave-functions of states with different spins unequal. As a consequence their contributions to the hyperfine fields at the nuclei do not vanish and have to be taken into account. The contribution from the exchange polarization effect is difficult to evaluate from first principles [36,37], particularly for large and complicated molecules of the present type. However, for the case of an unpaired π-electron on the carbon atom in a C-H bond, a semi-empirical relation is available [35] which gives the exchange polarization contribution to the proton hyperfine interaction constant, namely,

$$A_H = Q\rho^\pi \tag{10}$$

where ρ^{π} is the unpaired spin population on the π-orbital on the carbon atom and Q is about -70 MHz. This formula will be used to evaluate the exchange polarization effect for the methine protons where it is of crucial importance. For the other protons of interest, particularly the protons of rings II and IV, where the direct contribution from Eqn. 9 is substantial, the exchange polarization effect is not as crucial in importance and we shall only consider it qualitatively in discussing our results in the next section.

The second problem that has to be faced is that for the methyl protons, we need the average over rotating CH_3 groups which would require a set of time-consuming wave-function calculations for each different configuration of the rotating CH_3 groups. To avoid this problem, we shall make use of a semi-empirical expression which has been developed [38] relating the proton hyperfine constant A_H for the protons of the rotating methyl group to the unpaired spin population in the π state of the ring carbon atom bonded to the methyl group. This relation is based upon the idea that there is finite unpaired spin population appearing at the protons of a CH_3 group through hyperconjugation interaction between the unpaired π-orbital on the adjacent carbon atom and the C-H bonds of the methyl group. The semi-empirical expression is given by [15,38]:

$$A_H = (B_0 + B_1 \cos^2\theta)\rho^{\pi} \tag{11}$$

where $B_0 = 30$ MHz and $B_1 = 300$ MH_z are emperical parameters, θ is the angle between the plane involving the C-C and C-H bonds and that involving the π-orbital and the C-C bond. Since the parameters B_0 and B_1 are obtained empirically, one could consider that the influence of any exchange polarization effects present is included indirectly in Eqn. 11.

(III) Results and discussion

The unpaired spin population distribution over BPh^+ *a* and BPh^- *a* ions using our calculated wave-functions are shown in Figs. 4 and 5, respectively. In both systems, for the C, N and O atoms, both the net unpaired spin population arising from the 2s, $2p_x$, $2p_y$ and $2p_z$ orbitals as well as those from only the $2p_z(\pi)$ orbitals are noted in Figs. 4 and 5, the spin populations in the π state being enclosed in parentheses. We shall now analyze the main features of these spin population distributions, starting first with the cation.

(A) Unpaired spin population distribution and proton hyperfine constants in the cation, BPh^+ a

It can be seen from Fig. 4 for the spin population distribution in BPh^+ *a* that in addition to the significant unpaired spin populations at the carbon and nitrogen atoms in the earlier π-orbital calculations [20,21], there are sizable spin densities at a number of other atoms in the molecule. Thus, in the fifth ring and its side chains it can be seen from Fig. 4 that there are very significant unpaired spin populations on the oxygen atoms with the unpaired spin population carried in one of them (33) by the π-orbital and in two other (34 and 35)

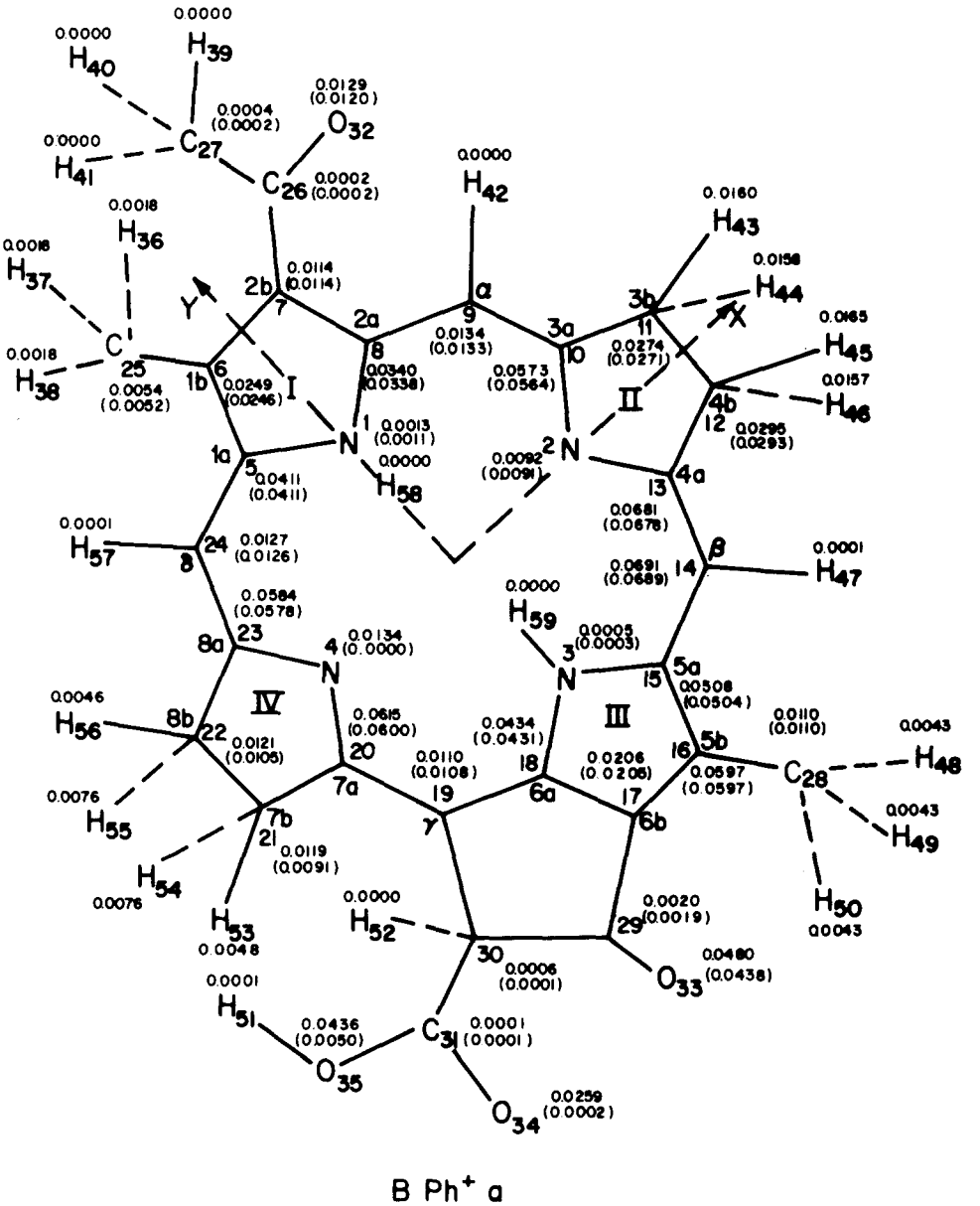

Fig. 4. Distribution of unpaired spin populations over the atoms in BPh^+ *a*. The numbers within parentheses for carbon, nitrogen and oxygen atoms represent the unpaired spin populations arising from the $2p_z(\pi)$ atomic orbital components of these atoms in the unpaired spin molecular orbital wave function.

by the other p-orbitals. There is also significant spin density on the oxygen atom in the CH_3-C=O attached to ring I. As a consequence of the distribution of the unpaired spin population over the other atoms in the molecule, there is a decrease in the unpaired spin populations on the carbon atoms which constitute the π-network, relative to the corresponding populations on these atoms from π-orbital calculations [20,21].

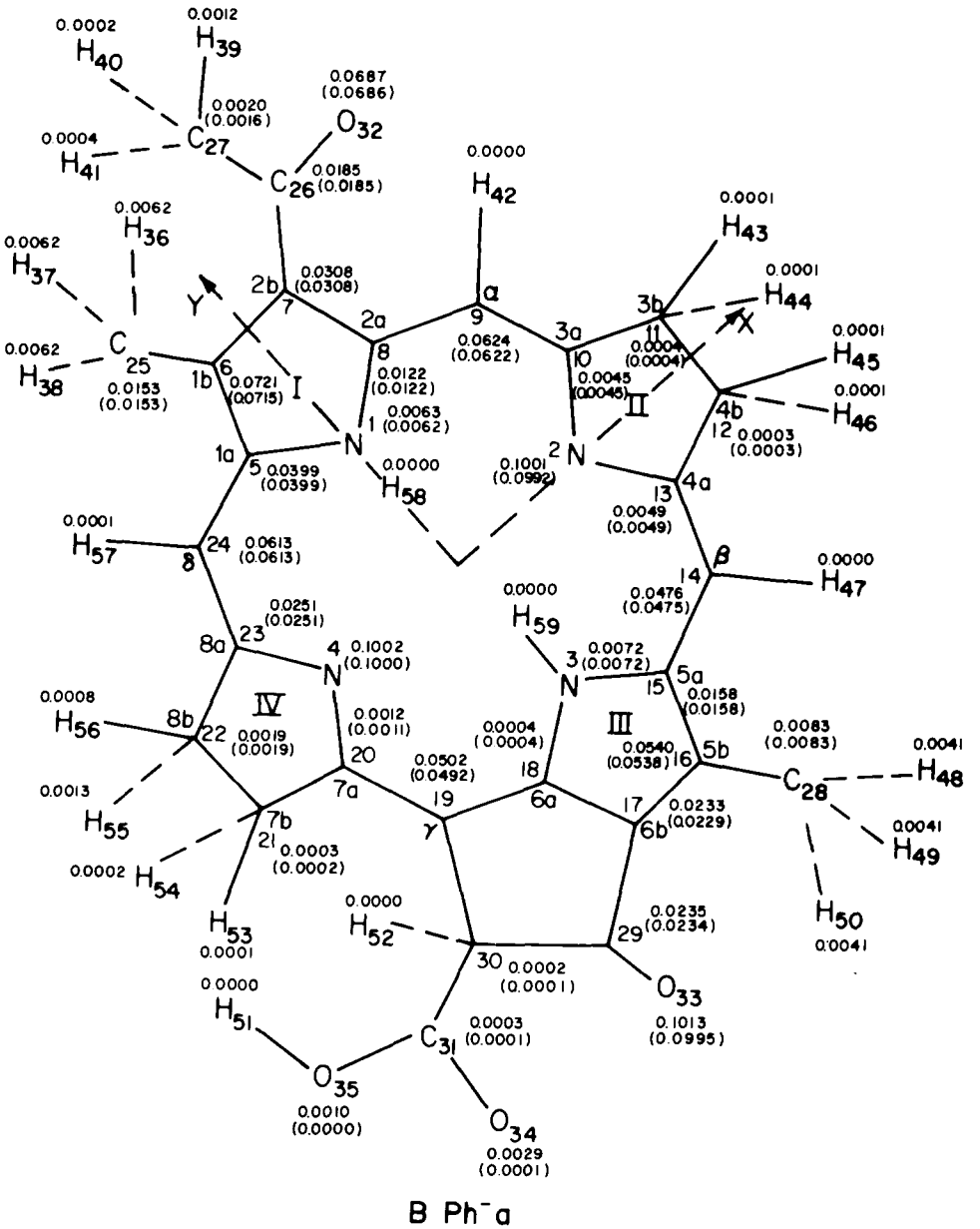

Fig. 5. Distribution of unpaired spin populations over the atoms in BPh^- *a*. The numbers within parentheses have the same meaning as in Fig. 4.

The most important feature of the spin population distribution in Fig. 4 obtained from our calcultions is the substantial difference in the spin populations in rings I and III. In particular, the unpaired spin populations on the carbon atoms in ring III are larger than on the corresponding carbon atoms in ring I. This larger unpaired spin population in ring III is most likely a consequence of the presence of the adjacent ring V, which in drawing spin popula-

TABLE I

THEORETICAL PROTON HYPERFINE CONSTANTS [a] in BPh^+ *a* AND BPh^- *a* COMPARED WITH EXPERIMENTAL RESULTS [b]

M Proton	Cation						Anion			
	Theoretical	Experimental					Theoretical	Experimental		
	BPh^+ *a*	BPh^+ *a*		$BChl^+$ *a*			BPh^- *a*	BPh^- *a* Ref. 17 [l]	$BChl^-$ *a*	
		Ref. 17 [g]	Ref. 15 [h]	Ref. 15 [i]	Ref. 16 [j]	Ref. 17 [k]			Ref. 40 [m]	Ref. 15 [n]
Methyl group ring I	+4.43	5.4	6 [p]	5.0 ± 0.1	5.32	4.78	+13.45	8.4	9.24	8.1
Methyl group ring III	+10.75	9.4		9.2 ± 0.2	9.8	9.44	+10.08	8.4	8.68	8.1
Ring IV protons [c,d,e]	+12.61					11.48	+0.35			
	+20.08					12.92	+0.56			
	+20.01			1.6	14.0	13.48	+3.99	<2.8	<2.8	
	+12.40					16.38	+2.60			
Methine protons [f]	−0.93						−4.52		7.0	
	−0.73	1.0			1.4	1.52	−4.29	7.0	5.6	
	−4.75						−3.46			

[a] The hyperfine constants are all expressed in MHz. In those cases where the experimental results are given in G from EPR or ENDOR measurements, we have converted them into MHz by multiplying by the conversion factor of 2.8 MHz per G.

[b] The values quoted for the experimental hyperfine constants refer only to their magnitudes since the signs have not been determined.

[c] The four theoretical hyperfine constants listed for ring IV in both the anion and cation refer to hydrogens 53, 54, 55 and 56 in the model system in Fig. 3.

[d] The experimental upper limits listed for the ring IV hyperfine constants in BPh^- *a* and $BChl^-$ *a* are from Fajer et al. [41] the proton hyperfine ENDOR pattern associated with the protons of ring II and ring IV being unresolved.

[e] The experimental proton hyperfine constants listed in the rows for ring IV for BPh^+ *a* and $BChl^+$ *a* refer actually to the protons of both rings II and IV. The reasons for comparing them with only the theoretical hyperfine constants ring IV are connected with the form of the ring in the model system chosen in Fig. 2, related to the methyl pheophorbide structure as discussed in Section II of this paper and in ref. 25.

[f] The theoretical methine hyperfine constants listed refer to hydrogen atoms α, δ and β, respectively, for both the anion and cation.

[g] Temperature, 298K.

[h] Temperature, 80K.

[i] Temperature, 80K.

[j] Temperature, 25K.

[k] Temperature, 273K.

[l] Temperature, 273K.

[m] Temperature, 240K.

[n] Temperature, 80K.

[p] Only one pair of peaks were observed in the ENDOR pattern of BPh^+ *a* in ref. 15. We have listed under ring I, in view of its being closer to the methyl group hyperfine constant in ring I rather than ring III.

tion towards itself also increases the spin population on ring III as compared to ring I which does not have an adjacent ring similar to V. The larger spin population in ring III, particularly on the carbon atom 5b bonded to the methyl group as compared to that on the corresponding carbon atom 1b in ring I, is of course very important from an experimental point of view because it can explain the larger hyperfine constant [15,17] associated with the protons of the methyl group bonded to ring III as compared to that for ring I. Thus, using the unpaired spin populations on atoms 1b and 5b in Eqn. 11 for the rotating methyl groups, the proton hyperfine constants for rings I and III are obtained as 4.43 and 10.75 MHz, respectively *. These values are compared with the corresponding values from ENDOR measurements for these protons in BPh^+ *a* and $BChl^+$ *a* in Table I. The values of these hyperfine constants predicted by theory can be seen to be in good agreement with experiment, the theoretical ratio $A_H(III)/A_H(I)$ for the CH_3 proton hyperfine interactions in the two rings being 2.4 as compared to 1.84—1.97 found experimentally in [15—17] $BChl^+$ *a* and [17] 1.74 in BPh^+ *a*.

Turning next to the unpaired spin populations on rings II and IV in Fig. 4, it is the spin density in ring IV that is meaningful to compare with experimental data in BPH^+ *a* and $BCHl^+$ *a* because both the rings IV and II are reduced in these systems while for the methylpheophorbide structure [25] that we have used (Section II), the positions of the carbon atoms in ring II were characteristic of an aromatic ring. The spin densities at the carbon sites 3b and 4b in ring II were found to be significantly larger than the corresponding carbons 7b and 8b in ring IV. This is likely consequence of the planar geometry of the aromatic ring II in methyl-pheophorbide structure, which allows a greater delocalization of the unpaired molecular orbital through it. One could use the spin populations in ring II to interpret hyperfine data in chlorophyll$^+$ *a* (Chl^+ *a*) free radical [16], except for the fact that we have two protons each attached to carbons 3b and 4b, in the model compound (Fig. 3) we have studied, in place of the CH_3 and C_2H_5 groups in Chl^+ *a*. Nevertheless, as a rough check of the calculated spin populations in ring II in Fig. 4, we can use the unpaired spin population on the carbon atom at 3b in combination with Eqn. 11 for an attached rotating CH_3 group to obtain 4.1 MHz for the hyperfine constant of the methyl protons, a value that is comparable to the experimental result in Chl^+ *a*. Also, this theoretical value, in keeping with experiment [16], is closer to the methyl group hyperfine constant in ring I of BPh^+ *a* than that for ring III.

The spin densities found on the protons in ring IV using the procedure described in Section IIB, can be converted into hyperfine constants using Eqn. 9. By this procedure, as can be seen from Table I, we get proton hyperfine constants of 12.6 and 20.1 MHz from the pair of protons in positions 53 and 54 and the very similar results 20.0 and 12.4 MHz from the proton pair 55 and

* The spin populations on these methyl hydrogen atom sites (36, 37 and 38 in ring I and 48, 49 and 50 in ring III) listed in Fig. 4 are in keeping with the calculated proton hyperfine constants 4.43 and 10.75 MHz. The spin populations at these hydrogen atoms are obtained using the calculated hyperfine constants together with Eqn. 9 and taking into account the fact that the wave-function for the unpaired electron indicates that the spin denstity at each of these proton sites gets about 60% contribution from the hydrogen atom ls orbitals and the balance from the tails of the 2p orbitals of the carbon atom of the methyl group.

56, respectively. Now, in making comparisons with experiment [15,17], we have to remember that in the model system we have used, one each of the hydrogen atoms in the pairs (53, 54) and (55, 56) is a replacement for a CH_3 group and a phytyl chain and, therefore, there are only two protons in ring IV directly attached to carbons 7b and 8b in BPh^+ *a* and $BChl^+$ *a*. It is, therefore, more meaningful to compare the average of the calculated proton hyperfine constants in ring IV with the experimental hyperfine constants for this ring. There are no measured values available in BPh^+ *a* itself, but in $BChl^+$ *a* the proton hyperfine constants for rings II and IV range [17] from 11.48 to 16.38 MHz in good agreement with the average value of 16.3 MHz from our results for the protons at sites 53, 54, 55 and 56. What is also important is that the order of the theoretical results from Table I show the same sequence for the proton hyperfine constants in rings I, III and IV as the experimental results [15—17] for these rings and the theoretical and experimental values of the respective ratios are also in reasonably good agreement.

We consider next the hyperfine constants associated with the methine protons attached to the α, β and δ carbons. The spin populations associated with the unpaired electron wave-function are seen from Fig. 4 to be very small at these proton sites. The fact that these spin populations are negligible but non-vanishing (0.0001) for the protons adjacent to the β and δ methine carbons is a consequence of the departure from planarity of the molecule. The proton hyperfine constants associated with the spin densities at the β and δ methine proton sites are seen from Eqn. 9 to be quite small, only 0.07 and 0.15 MHz, respectively. However, as mentioned already in Section II, there can be larger contributions from the exchange polarization effect [35] associated with the unpaired spin polarization on the adjacent carbon atoms. The spin populations on the α and δ methine carbons are seen from Fig. 4 to be nearly equal and about a fifth of the spin population on the β methine carbon. From a consideration of the relative positions (Fig. 4) of the α, β, and δ methine carbons with respect to the rings I—V in the molecule, the similarity between the α and δ methine carbons and their difference from the β methine carbon become understandable. Thus, the α and δ methine carbons lie on either side of the ring I, the β methine carbon is adjacent to ring III which has the ring V linked to it.

Using Eqn. 10 relating the spin population on the carbon atom to $A_H(EP)$, the exchange polarization (EP) contribution to the hyperfine constant of the proton in a methine bond. $A_H(EP)$ for the α and δ protons come out as —0.93 MHz and —0.88 MHz, respectively, while for the β proton, $A_H(EP)$ comes out as —4.82 MHz. On combining with the contributions to the α, β and δ methine proton hyperfine constants from the spin population directly contributed to by the unpaired electron, we get the theoretical hyperfine constants listed in Table I. Of these, the α and δ methine proton hyperfine constants agree well with the observed experimental value associated with the methine protons in BPh^+ *a*, which is somewhat smaller than the corresponding experimental value [16,17] in $BChl^+$ *a*.

Considering the β methine proton, there is no experimental evidence currently available for an additional ENDOR frequency of comparable size as the theoretical value of —4.75 MHz associated with the methine protons. There could be a number of reasons for this. One possibility is that there may be sub-

stantial anisotropy in the hyperfine field due to the electron-nuclear dipole interaction associated with the large spin population on the carbon atom of the β methine bond. The other possibility is that the value of A_H associated with the β methine proton is comparable to that of the methyl group protons in ring I and its ENDOR spectrum could, therefore, be hidden within the linewidth of the ring I proton ENDOR line. It would be very useful from the view of testing the theory if some experimental technique could be found to measure the A_H associated with the β methine proton.

(B) Unpaired spin population distribution and proton hyperfine constants in the anion, BPh^- a

We consider next the results of our calculation for the spin population distribution in the anion, BPh^- *a*, the predicted hyperfine constants for the protons and their comparison with experimental results as well as with the theoretical and experimental results for the cation, BPh^+ *a*. The first and a very important feature of the spin distribution in the anion in Fig. 5 in reference to experimental results on the proton hyperfine data, is that the spin population distributions in rings I and III are reasonably close to each other in contrast to the situation in Fig. 4 for the cation, where the spin populations on the carbon atoms 1b and 2b in ring I were smaller by a factor a little over 2 as compared to those on the corresponding carbon atoms 5b and 6b, respectively, in ring III.

The spin populations on the α and δ methine carbon atoms in the anion are seen to be almost five times larger than in the cation. For the β methine carbon, the spin population is comparable to those for the α and δ methine carbons and similar to that for the β methine carbon in the cation. That is, for the three methine carbons at α, β and δ positions in the anion, the unpaired spin populations are all comparable, in contrast to the case of the cation where our results show that these populations differ by a factor of five between the α and δ methine carbons on the one hand and the β methine carbon on the other.

As far as rings II and IV are concerned, the unpaired spin populations in the anion are seen from Fig. 5 to be rather small compared to those in rings I and III, in contrast to the situation in the cation in Fig. 4 where the spin populations in rings II and IV are substantially larger than in rings I and III. The smallness of the spin populations in rings II and IV in the anion relative to the cation can be noted by comparing, in the two cases, the spin populations at the hydrogen sites, which produce the proton hyperfine constants. Thus the largest spin population at the hydrogen atom site (H 55) in ring IV in the anion is seen to be about a sixth of the corresponding population in the cation.

Finally, for ring V, one can see from Figs. 4 and 5 that the overall spin population distributions in the cation and anion are very similar except for differences in detail in the populations on some of the atoms. This similarity is important to notice in attempting to understand the origin of the redistribution of spin populations over the anion as compared to the cation. Thus, since the net spin population per unpaired electron is unity, the increase in spin population in one region of the molecule must occur at the expense of that in another region. It can be seen from the spin distributions in the cation and anion in Figs. 4 and 5 that for the two different unpaired states in the two systems, the net spin populations over the rings III and V do not change very much. It

appears as if the two rings III and V being linked to each other act as stabilizing factors on each other for the electronic distribution. One could thus consider that the increase in the spin populations in ring I and at the α and δ methine groups in the anion, relative to the cation, occurs at the expense of the rings II and IV which in the anion have lost spin populations very significantly relative to the cation. The theoretical study of the spin distributions in the two systems thus shows that the trends of changes [15—18] in the hyperfine constants for different parts of the molecules in going from the cation to the anion are related, the picture of the redistribution process for the spin population being the following. The rings III and V appear to retain their spin population in going from cation to anion, the associated proton hyperfine constant for the rotating methyl group in ring III being observed to remain unchanged [15—18] as well. The rings II and IV as seen from Figs. 4 and 5 to lose their spin populations severely, with the spin populations and the observed proton hyperfine constants going from a situation where they are the largest for the cation to one where they are the smallest for the anion. The beneficiaries of the loss of spin population in the anion from rings II and IV are the ring I and the methine groups α and δ. The increase in the spin populations on ring I increases the proton hyperfine constant for the rotating methyl group attached to carbon atom 1b from a situation in the cation [15] where it is about one-half of that for protons in the rotating methyl group attached to ring III to the point where in the anion [14,17], it is comparable to (and theoretically from the present work, a little larger than) the latter.

In the second half of Table I, we have listed the calculated hyperfine constants in the anion for the methyl protons attached to rings I and III, the protons in the methine groups α, β and δ and the protons in rings II and IV and compared them with experiment [15,18]. As was done in Section IIIA for BPh^+ *a*, these theoretical values represent the direct contributions from the unpaired valence electron in the case of all the protons except the methine protons, Eqn. 9 being used for obtaining the proton hyperfine constants for the protons of rings II and IV and Eqn. 11 for the protons of the rotating methyl groups attached to rings I and III. For the methine protons, as remarked before, the direct contributions from the unpaired spin electron are very small. Consequently the major contribution arises from the exchange polarization effect [31—35], for which Eqn. 10 [35] has been used. While we have included the sign of the hyperfine constant in our theoretical results, one is unable to obtain them experimentally from ENDOR measurements [39] which provide splittings in frequency.

The comparison between the theoretical and experimental [18] trends in the hyperfine constants for different protons within the anion, and also as compared to the cation [15—17], have already been discussed earlier in this section while discussing the spin population distributions. The theoretical ratio of the proton hyperfine constants in BPh^- *a* for the methyl groups attached to rings III and I is seen to be about 0.75 as compared to the near equality from experimental results. But this difference * between theory and experiment is rela-

* Professor G. Feher (personal communication) has informed us that from measurements by his group, the ENDOR line associated with the methyl protons of ring I and III is asymmetric indicating that it may be composed of two lines of different frequency. Dr. J. Fajer and collaborators (see ref. 40) have obtained difference between the frequencies of the two proton ENDOR lines in $BChl^-$ *a*, although the difference is somewhat smaller (about 10% or smaller) than the 25% we find from theory.

tively small, when compared to the corresponding theoretical ratio of 2.4 from our calculations in BPh^+ *a* and experimental ratios of 1.74 in the same compound [18] and [15—17] 1.84—1.97 in $BChl^+$ *a*. As emphasized earlier, the important aspect of the present theoretical analysis is that using the same procedure for obtaining the electronic wave-functions in the cation and anion, one can explain both the observed vastly different values of the methyl proton hyperfine constants in rings I and III in the cation [15—17] and the closeness of the corresponding quantities in the anion [18]. Our theoretical results in Table I are also seen to provide agreement with the observed features [18] of substantially large hyperfine constants in the anion for the methine protons and relatively small ones for the protons of rings II and IV. As regards the absolute magnitudes of the proton hyperfine constants, the agreement between theory and experiment is also seen to be quite reasonable considering the semi-empirical nature of the procedure [22—24] employed to obtain the electronic wave-functions and the Eqns. 10 and 11 used to obtain the proton hyperfine constants for the methine and rotating methyl groups.

Before completing this section we shall remark on the hyperfine constants associated with the other protons besides those observed experimentally. The only other protons besides the ones we discussed so far in the model system in Fig. 3 that we have chosen for BPh *a* are the protons 39, 40 and 41 in the CH_3-C=O group attached to ring I and those in the hydrogen atoms 51 and 52 in ring V. Of these, the hydrogen atom at position 51 does not exist in the real BPh^+ *a* and BPh^- *a* molecules, because it is a replacement for a CH_3 group. For the cation, the spin population at the carbon atom (No. 26) of the C=O group adjacent to the CH_3 is seen to be very small and, therefore, using Eqn. 11 one does not expect significant hyperfine interaction for the methyl protons 39, 40, 41. For the hydrogen atom No. 52, the calculated spin density is very small as also is the spin population on the adjacent carbon atom. Therefore, both the direct and exchange polarization contributions to the proton hyperfine constant for this hydrogen atom are negligible. It appears then that with the possible exception of the β methine protons, the protons expected to have significant hyperfine interaction in BPh^+ *a* have been accounted for experimentally.

For the anion the significant spin population in ring I is seen from Fig. 5 to lead to a sizable spin population on the CH_3-C=O group attached to carbon atom 2b. Using the calculated spin population on the carbon atom (No. 26) of the C=O group and Eqn. 11, we obtain 3.3 MHz for the hyperfine constant for the protons of the methyl group assuming the latter to be rotating as was the case for the other methyl groups. There is no experimental evidence available for this proton hyperfine constant but its size indicates that it could be amenable to observation in the future. For the hydrogen atom No. 52, the proton hyperfine constant is again expected, from the spin populations in Fig. 5 to be rather small due to the same reasons as pointed out for the cation in the preceding paragraph.

Conclusion

The unusually rich insight that ENDOR measurements have provided [15—18] into electronic distribution over positive and negative ion radicals of

bacteriochlorophyll and bacteriopheophytin has been used to test the theoretical understanding of the electronic structures of these systems by making comparisons between predicted hyperfine constants from theory with experimental data. It is shown that a molecular orbital procedure applied to bacteriopheophytin free radical systems, both cation and anion, including explicitly both π and σ atomic orbitals and incorporating fully the atomic orbitals of all the five rings I—V, not only leads to good overall agreement in magnitude with experimental proton hyperfine data [15—19] but can also explain differences in the proton hyperfine constants within both the cation and anion and the interrelationships of the hyperfine data in the two systems. The most notable of the experimental trends that is explained by the theory is the substantially different methyl proton hyperfine constants in rings I and III in the cation [15—17] and nearly equal hyperfine constants in the anion [15—18]. The success in explaining this and other trends in the proton hyperfine data, as well as a reasonable explanation of their magnitude, indicates that theory has provided a good understanding of the electronic distributions in these monomer ions which could be used to further enhance our knowledge of the aspects of these systems that are important for the process of photosynthesis, for example the nature of the bonding [10—13] of the monomers to form dimers.

Our theoretical analysis indicates the presence of substantial spin populations on the atoms of the fifth ring and its ligand in both BPh^+ *a* and BPh^- *a*. Some of these spin population appears on the oxygen atoms in ring V indicating that there should be significant hyperfine fields at the oxygen nuclear sites. It would be very helpful to explore these hyperfine fields through the ENDOR pattern of ^{17}O nuclei. Also, to continue to improve the understanding of the electronic structures of these systems, in the future it will be helpful to theoretically study the electronic structure of the bacteriochlorophyll cation and anion by the same procedure as we have adopted for the bacteriopheophytin system here and in earlier work. While the proton hyperfine constants in the bacteriochlorophyll cation [15—17] and anion [15,18] are observed to be very similar to their bacteriopheophytin counterparts, and follow the same trend in going from the cation to the anion, there are small but significant differences referred to already in the introduction (Section I), that could be related to the interaction in bacteriochlorophyll between the magnesium atom and the rest of the system.

References

1 Bolton, J.R., Clayton, R.K. and Reed, D.W. (1969) Photochem. Photobiol. 9, 209—218
2 McElroy, J.D., Feher, G. and Mauzerall, D.C. (1969) Biochim. Biophys. Acta 172, 180—183
3 McElroy, J.D., Feher, G. and Mauzerall, D.C. (1972) Biochim. Biophys. Acta 267, 363—374
4 McElroy, J.D., Mauzerall, D.C. and Feher, G., (1974) Biochim. Biophys. Acta 333, 261—278
5 Feher, G., Hoff, A.J., Isaacson, R.A. and McElroy, J.D., (1973) Biophys. Soc. Abstr. 13, 61
6 Norris, J.R., Druyan, M.E. and Katz, J.J. (1973) J. Am. Chem. Soc. 95, 1680—1682
7 Norris, J.R., Uphaus, R.A., Crespi, H.L. and Katz, J.J. (1971) Proc. Natl. Acad. Sci. U.S. 68, 625—628
8 Debrunner, P.G., Schulz, C.E., Feher, G. and Okamura, M.Y. (1975) Biophys. J. 15, 226a
9 Okamura, M.Y., Isaacson, R.A. and Feher, G. (1975) Proc. Natl. Acad. Sci. U.S. 72, 3491—3495
10 Katz, J.J. and Norris, J.R. (1973) in Current Topics in Bioenergetics (Sanadi, D.R. and Packer, L., eds.), Vol. 5, pp. 41—75, Academic Press, New York
11 Fong, F.K. (1975) Theory of Molecular Relaxation, Chapt. 9, Wiley-Interscience, New York
12 Shipman, L.L., Cotton, T.M., Norris, J.R. and Katz, J.J. (1976) Proc. Natl. Acad. Sci. U.S. 73, 1791—1794

13 Boxer, S.G. and Closs, G.L. (1976) J. Am. Chem. Soc. 98, 5406—5408
14 Fajer, J., Brune, D.C., Davis, M.S., Forman, A. and Spaulding, L.D. (1975) Proc. Natl. Acad. Sci. U.S. 72, 4956—4960
15 Feher, G., Hoff, A.J., Isaacson, R.A. and Ackerson, L. (1975) Ann. N.Y. Acad. Sci. 244, 239—259
16 Norris, J.R., Scheer, H. and Katz, J.J. (1975) Ann. N.Y. Acad. Sci. 244, 260—280
17 Borg, D.C., Forman, A. and Fajer, J. (1976) J. Am. Chem. Soc. 98, 6889—6893
18 Fajer, J. (1977) Biophys. J. 17, 150a
19 Feher, G. (1977) Biophys. J. 17, 149a
20 Fajer, J., Borg, D.C., Forman, A., Felton, R.H., Dolphin, D. and Vegh, L. (1974) Proc. Natl. Acad. Sci. 71, 994—998
21 Otten, H.A. (1971) Photochem. Photobiol. 14, 589—596
22 Hoffman, R. (1963) J. Chem. Phys. 39, 1397—1412
23 Zerner, M., Gouterman, M. and Kobayashi, H. (1966) Theor. Chim. Acta (Berl.) 6, 363—400
24 Han, P.S., Das, T.P. and Rettig, M.F. (1970) Theor. Chim. Acta (Berl.) 16, 1—21
25 Fischer, M.S., Templeton, D.H., Zalkin, A. and Calvin, M. (1972) J. Am. Chem. Soc. 94, 3613—3619
26 Pauling, L. (1948) The Nature of the Chemical Bond, Cornell University Press, Ithaca, New York
27 Sutton, C.E. (1958) Tables of Interatomic Distances and Configurations in Molecules and Ions, Special Publication No. 11, The Chem. Society, London, Burlington House, W.I.
28 Mulliken, R.S. (1955) J. Chem. Phys. 23, 1833—1846
29 Carrington, A. and McLachlan, A.D. (1967) Introduction to Magnetic Resonance, Harper and Row, New York
30 Fermi, E. (1930) Z. Phys. 60, 320—333
31 Das, T.P. (1973) Relativistic Quantum Mechanics of Electrons, Chapt. 7, Harper and Row, New York
32 Gaspari, G.D., Shyu, W.M. and Das, T.P. (1964) Phys. Rev. 134, A852—A862
33 Mahanti, S.D., Tterlikkis, L. and Das, T.P. (1970) in Magnetic Resonance, (Coogan, C.K., Ham, N.S., Stuart, S.N., Pilbrow, J.R. and Wilson, G.V.H., eds.), pp. 91—118, Plenum Press, New York
34 Watson, R.E. and Freeman, A.J. (1967) in Hyperfine Interactions (Freeman, A.J. and Frankel, R.B., eds.), Chapt. 2, Academic Press, New York
35 McConnell, H.M. (1956) J. Chem. Phys. 24, 764—766
36 Poling, S.M., Davidson, E.R. and Vincow, G. (1971) J. Chem. Phys. 54, 3005—3013
37 Rodgers, J.E., Lee, T., Das, T.P. and Ikenberry, D. (1973) Phys. Rev. A7, 51—59
38 Wertz, J.E. and Bolton, J.R. (1972) Electron Spin Resonance, Chapt. 8, (and references therein), McGraw-Hill, New York
39 Feher, G. (1957) Phys. Rev. 105, 1122—1123
40 Fajer, J., Forman, A., Davis, M.S., Spaulding, L.D., Brune, D.C. and Felton, R.H. (1977) J. Am. Chem. Soc. 99, 4134—4140
41 Fajer, J., Davis, M.S., Brune, D.C., Spaulding, L.D., Borg, D.C. and Forman, A. (1976) Chlorophyll-Proteins, Reaction Centers and Photosynthetic Membranes, Brookhaven Symposia in Biology, No. 28, pp. 74—104